Robust and Fast Voltage-Source-Converter (VSC) Control for Naval Shipboard Microgrids

Heydari, Rasool; Gheisarnejad, Meysam; Khooban, Mohammad Hassan; Dragicevic, Tomislav; Blåbjerg, Frede

Published in:
IEEE Transactions on Power Electronics

DOI (link to publication from Publisher):
10.1109/TPEL.2019.2896244

Publication date:
2019

Document Version
Accepted author manuscript, peer reviewed version

Robust and Fast Voltage-Source-Converter (VSC) Control for Naval Shipboard Microgrids

Rasool Heydari, *Student Member, IEEE,* Meysam Gheisarnejad, Mohammad Hassan Khooban, *Senior Member, IEEE,* Tomislav Dragicevic, *Senior Member, IEEE,* and Frede Blaabjerg, *Fellow, IEEE*

***Abstract*—This paper proposes a new modified model predictive control to compensate for voltage and frequency deviations with higher bandwidth for an AC shipboard microgrid. The shipboard power system (SPS) and islanded microgrids (MGs) have a reasonable analogy regarding supplying loads with local generations. However, a great number of vital imposing pulse loads and highly dynamic large propulsion loads in the SPS make the frequency and voltage regulation a complicated issue. Conventional linear control methods suffer from high sensitivity to parameter variations and slow transient response, which make big oscillations in the frequency and voltage of the SPS. This paper addresses the problem by proposing a novel finite control set model predictive control to compensate for primary frequency and voltage deviations with higher bandwidth and order of magnitude faster than state of the art. Furthermore, a single input interval type-2 fuzzy logic controller (SI-IT2-FLC) is applied in secondary level to damp the steady-state deviations with higher bandwidth. Finally, hardware-in-the-loop (HiL) experimental results prove the applicability of the proposed control structure.**

***Index Terms*—Finite control set, model predictive control, shipboard power system (SPS), Fuzzy logic controller (FLC)**

I. Introduction

SHIPBOARD power systems (SPSs) have been operated for decades as a mobile islanded microgrid (MG). In the following century, the SPS has evolved significantly in power level and electric propulsion loads. Therefore, the presence of large propulsion loads and power electronic converter interfaces lead to severe frequency and voltage control issues in the SPS. A large pulsed power load (PPL) in a SPS deviates the frequency dramatically, so that fast, accurate and robust control structure is a highly desirable feature.

A comprehensive model of the SPS is presented in [1] where an adaptive and time-varying controller is presented for the load-frequency control in a SPS. However, the transient performance of the frequency and voltage control is not acknowledge. Furthermore, high bandwidth control strategy is not considered. In this regards, hierarchical control structures have been applied for the control of the voltage and frequency [2], [3]. At the primary control level, multi-loop linear PI controllers are conventionally employed to control the output voltage and current of converter locally. At the upper level, the secondary control compensates for voltage and frequency deviations caused by the primary control level. In this control structure, in order to avoid undesired interaction, each outer loops should be designed with lower bandwidth compared to the inner loops [4]. Therefore, this control strategy suffers from the slow dynamic response and sluggish transient performance. In [5], a dynamic decoupling between the output capacitor voltage and inductor current is presented in the primary control level to increase the bandwidth of the SPS. However, this control model is not fast enough to recover deviated frequency and voltage during the transient.

Recently, a model predictive control (MPC) approach is presented for the control of the power converters [6]–[8]. A new high bandwidth control structure has been presented in [9], where a finite control set MPC strategy is employed at primary control level to increase the bandwidth of the control system. However, the secondary controller is not tune analytically. Furthermore, stability analysis is not acknowledged properly. In [10] a FCS-MPC and PI controller are employed at primary and secondary control levels, respectively to increase the bandwidth of the control structure. However, low bandwidth controller is applied at secondary control level.

In this letter, a high bandwidth finite control set model predictive control (FCS-MPC) is presented for the SPS to compensate for the voltage and frequency deviations during the transient and steady state operation. Furthermore, a novel single input interval type-2 fuzzy logic controller is presented to regulate the SPS voltage and frequency with higher bandwidth. The major novelties of the letter are: 1) The new proposed control structure is much faster than linear cascaded control methods presented in the literature. 2) The frequency and voltage of the SPS are stable with higher bandwidth compared to the conventional methods. 3) Accurate power sharing is assured during transients and steady-states. 4) A new single input interval type-2 fuzzy logic controller (SI-IT2-FLC) is employed for secondary control level. Besides, experimental results illustrate the fast and accurate performance of the proposed approach compared to the state-of-the-art methods.

II. Shipboard AC Power System (SPS)

Fig. 1 presents a block diagram of a naval SPS. It comprises electronic PPL, and energy storage systems [11]. The SPS and the MG operation are controlled by the shipboard power management system (SPMS) and the ship dispatch system (SDS), respectively. Also, bidirectional information transfer can be achieved through communication links. Fig. 1 demonstrates an AC-SPS model consist of voltage source converters (VSCs) as an interface between energy storage systems (ESS) or energy resources and AC common bus. All small-scale RERs and energy storage units are connected to the AC bus via a circuit breaker and VSC with a LC filter. The spinning reserve for the secondary frequency control is provided by diesel ship power system. The small-signal analysis of the SPS is investigated in [1]. However, the slow dynamic response of conventional control structures are not addressed comprehensively. In order to have proper voltage and frequency regulation, the paralleled VSCs should be controlled fast and accurate to support the loads especially during transient with PPLs. In the following section, the proposed high bandwidth control structure is illustrated.

III. Proposed Predictive Control Strategy

Control structure plays a prominent role in reliable operation of the SPS, while there are a great number of vital imposing PPLs. Some of the loads are intermittent, operating on time scales down to milliseconds or less, and can range in power from small kW to vast MW which may reach 90% of the installed power capacity in a short period [12].

R. Heydari, T. Dragicevic and F. Blaabjerg are with the Department of Energy Technology, Aalborg University, Aalborg, DK, 9220, Denmark e-mail: (rah@et.aau.dk, tdr@et.aau.dk, fbl@et.aau.dk).

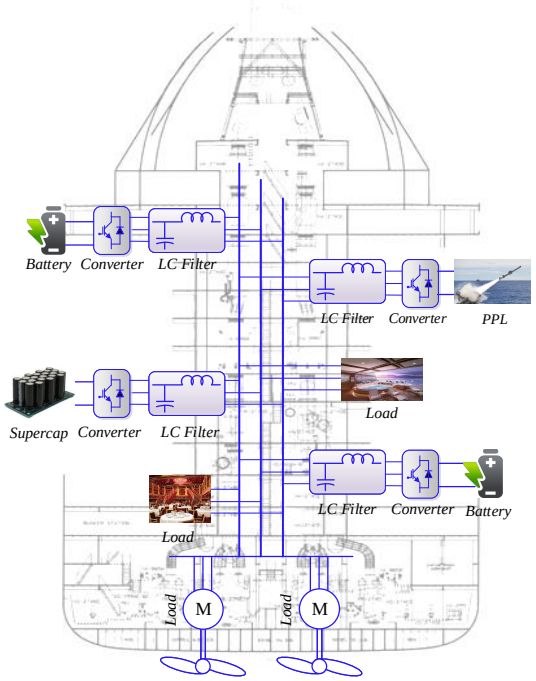

Fig. 1. Simplified model of VSCs connected to the SPS.

1) FCS-MPC structure: Three binary gating signals i.e. S_a, S_b, and S_c generate switching states of the two level three phase VSC. By employing a complex Clarke transformation, eight (2^3) switching configurations, in $\alpha\beta$ frame, are achieved. The main objective of the FCS-MPC is to appropriately adapt the input signals, so that, the output voltage follows the reference trajectory identically. Worth to note that a three phase LC filter is connected to each VSC to suppress the switching harmonics. The dynamic model of the SPS is demonstrated in Fig. 2. The output filter current (i_f) and the capacitor voltage (v_f) are the state variables of the SPS. The system model is based on the $\alpha-\beta$ reference frame, hence, three phase variable vector are transferred to the two dimensional space vector as follows:

$$\overline{z_\alpha} + j\overline{z_\beta} = T[z_u \quad z_v \quad z_w]', \tag{1}$$

where

$$T = \frac{1}{3}\begin{bmatrix} 1 & e^{j\frac{2}{3}\pi} & e^{j\frac{4}{3}\pi} \end{bmatrix}. \tag{2}$$

The filter current and capacitor voltage are measured, while the output current is being estimated using state observer. The controller presents a cost function (CF) and calculates the CF value for each of the discrete active vectors. Consequently, the vector for which the CF has a minimal value is applied to the VSC. In this structure, multi-loop linear voltage and current controller as well as PWM are replaced with a FCS-MPC controller. The CF can be formulated as follows [7]:

$$CF : \|\overline{v}_e(i)\|^2 + \xi_{lim}(i) + \zeta_w SW^2(i)) + G_d, \tag{3}$$

$$\overline{v}_e(i) = \overline{v}_f^*(i) - \overline{v}_e(i), \tag{4}$$

$$\xi_{lim}(i) = \begin{cases} 1, & \text{if } |i_f(i)| \leq i_{max} \\ \infty, & \text{if } |i_f(i)| > i_{max} \end{cases}, \tag{5}$$

$$SW(i) = \sum |u(i) - u(i-1)|, \tag{6}$$

$$G_d = \left(\frac{d\overline{v}_f^*(t)}{dt} - \frac{d\overline{v}_f(t)}{dt}\right) = (C_f\omega_{ref}v_{f\beta}^* - i_{f\alpha} + i_{o\alpha})^2 + (C_f\omega_{ref}v_{f\alpha}^* - i_{f\beta} + i_{o\beta})^2 \tag{7}$$

Where $v_e(i)$ illustrates the output error, $\overline{v}_f^*(i)$ is the reference output voltage and $\overline{v}_e(i)$ presents the predicted output voltage. Furthermore, $\xi_{lim}(i)$ shows the current constraint, $SW(i)$ represents switching effort with a weighting factor ζ_w and G_d shows the derivative voltage error. In this CF, current constraint and switching effort as well as voltage derivative error is added to the main CF, which follows the reference voltage. Therefore, current control loop also can be removed. For instance, if vector v_i produces the lowest value of the CF, then the voltage vector v_i is selected and applied in the VSC. On the other hand, if vector v_i produces a current, larger than the defined current limitation, the cost function CF would be infinite (since $\xi_{lim} = \infty$) and the voltage vector v_i would not be selected to apply in the VSC. Therefore, this FCS-MPC approach can limit the current during any fault and protect the semiconductor devices. The reference voltage $\overline{v}_f^*(i)$ can be determined through upper level droop control and virtual impedance.

IV. SI-IT2-FPI CONTROLLER

To compensate the voltage and frequency deviations and also to achieve a desirable gain margin to ensure the SPS stability in the steady state, the SI-IT2 fuzzy PI (SI-IT2-FPI) secondary controller was developed, as shown in Fig. 2. In the given structure, k_e is the input scaling factor (SF) of SI-IT2-FPI which normalizes the input to the universe of discourse where the membership functions (MFs) of the SI-IT2-FPI are characterized. Here, this SF is defined as $k_e = 1/e_{max}$ and e_{max} denotes the maximum value of error. The input to the SI-IT2-FPI (σ_o) is generated by normalizing the error. Then, the control signal (u_{pi}) is produced by the output of the SI-IT2-FI (φ_o) as:

$$u_{pi} = k_u(k_p\varphi_o + k_i\int \varphi_o dt) \tag{8}$$

where k_u is the output SF and is defined as $k_u = k_e^{-1}$, $\{k_p, k_i\}$ are the baseline PI controller gains.

A. Single Input Interval Type-2 Fuzzy Logic Controllers

The generic rule structure of each SI-IT2-FLC is described as:

$$R_n : \; if\, \sigma \; is \; \tilde{A_n}, Then\, \varphi_o \, is \, B_n \tag{9}$$

In the above rule, B_n denotes the crisp consequences which are defined as $B_1 = -1, B_2 = 0, B_3 = 1$. The antecedent MFs are defined by triangular IT2 fuzzy sets (IT2FSs) A_n, as depicted in Fig. 3. Compared to the type-1 fuzzy sets (T1FSs), an extra degree of freedom is provided by the IT2-FSs, called as footprint of uncertainty (FOU), and the sets are described in the terms of lower MF ($\mu_{\tilde{A_n}}$) and upper MF ($\overline{\mu_{\tilde{A_n}}}$). In Fig. 3, the coefficients of m_i (i=1, 2 and 3) denote the height of the lower MFs that construct the FOUs of the IT2-FSs. To simplify the design complexity, the symmetrical MFs are employed in the present work with the following assumptions:

$$m_1 = m_3 = 1 - \alpha \tag{10}$$

$$m_2 = \alpha \tag{11}$$

In the above equations, α is the only coefficient that should be adjusted in the IT2-FLC. The center of sets type reduction scheme is adopted in the SI-IT2-FLC, thus the output can be expressed as:

$$\varphi_o = ({\varphi_o}^r + {\varphi_o}^l)/2 \tag{12}$$

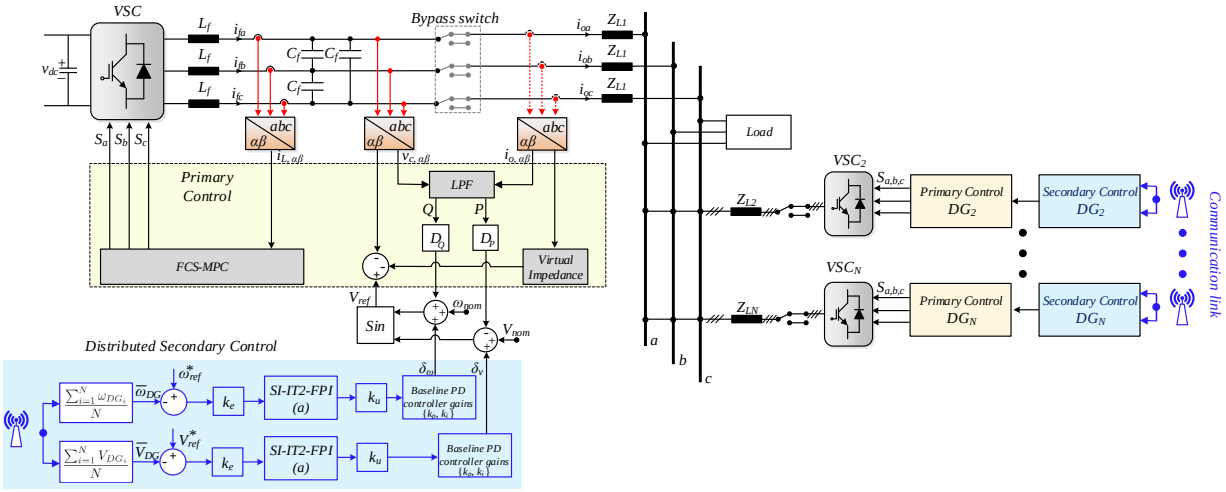

Fig. 2. Proposed dynamic scheme of control structure in SPS.

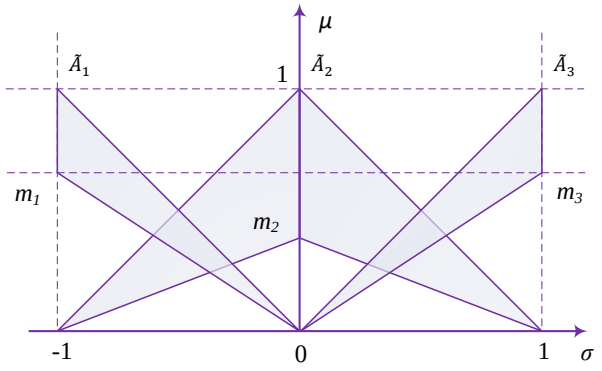

Fig. 3. Antecedent IT2-FSs of the IT2-FLC.

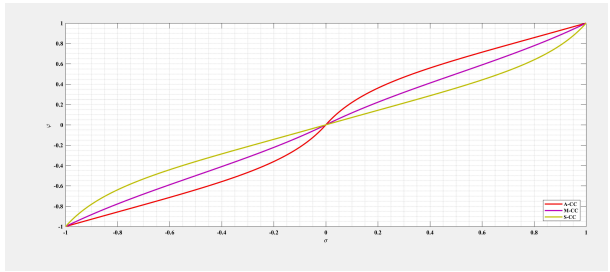

Fig. 4. Illustration of the A-CC, M-CC and S-CC.

where $\varphi_o{}^r$ and $\varphi_o{}^l$ represent the end points of the type reduced set which are calculated as:

$$\varphi_o^l = \frac{\sum_{(n=1)}^{L} \overline{\mu_{\tilde{A_n}}}(\sigma).B_n + \sum_{(n=L+1)}^{N} \underline{\mu_{\tilde{A_n}}}(\sigma).B_n}{\sum_{(n=1)}^{L} \overline{\mu_{\tilde{A_n}}}(\sigma) + \sum_{(n=L+1)}^{N} \underline{\mu_{\tilde{A_n}}}(\sigma)} \tag{13}$$

$$\varphi_o^r = \frac{\sum_{(n=1)}^{R} \underline{\mu_{\tilde{A_n}}}(\sigma).B_n + \sum_{(n=R+1)}^{N} \overline{\mu_{\tilde{A_n}}}(\sigma).B_n}{\sum_{(n=1)}^{R} \underline{\mu_{\tilde{A_n}}}(\sigma) + \sum_{(n=R+1)}^{N} \overline{\mu_{\tilde{A_n}}}(\sigma)} \tag{14}$$

Here, L and R are the switching points. The fuzzy mappings (FM) of the SI-IT2-FLC $\varphi_o()$ can be described as follows [13]:

$$k(\sigma) = \frac{1}{2}\left(\frac{1}{\alpha + \sigma - \alpha\sigma} + \frac{\alpha - 1}{\alpha\sigma - 1}\right) \tag{15}$$

B. Design scheme of the SI-IT2-FLC

Let $\varepsilon_o(\sigma) = \varphi_o(\sigma) - \sigma$, then three control curves (CCs) can be created by:

(i) Aggressive $CC(A - CC_{IT2})$: when $0 < \alpha \leq \alpha_{c1}$, then $\varepsilon > 0$ for $\forall\sigma \in [0, 1)$ and $\alpha_{c1} = (3 - \sqrt{5})/2$.

(ii) Smooth $CC(S - CC_{IT2})$: when $\alpha_{c2} < \alpha \leq 1$, then $\varepsilon < 0$ for $\forall\sigma \in [0, 1)$ and $\alpha_{c2} = (\sqrt{5} - 1)/2$.

(iii) Moderate $CC(M - CC_{IT2})$: when $\alpha_{c1} < \alpha \leq \alpha_{c2}$, then $\varepsilon < 0$ for $\forall\sigma \in [0.5, 1]$.

Fig. 4. illustrates the curves of the CCs, i.e. $A - CC_{IT2}$, $S - CC_{IT2}$ and $M - CC_{IT2}$, which are sketched under different values of α.$A - CC_{IT2}$ will has a high input sensitivity than $S - CC_{IT2}$ when ε is in the region close to zero. When the input signal is in the region close to ± 1, $S - CC_{IT2}$ will has a high sensitivity than $A - CC_{IT2}$. Lastly, $M - CC_{IT2}$ is formed by a mix of $A - CC_{IT2}$ and $S - CC_{IT2}$. Thus, $M - CC_{IT2}$ has a low sensitivity when the input signal is in the region close to ± 1, whereas it has a high sensitivity when the input signal is in the region close to zero. For more details about about the CCs specifications of the SI-IT2-FLC, the readers are referred to [14].

V. Experimental Results

In order to verify the fast and accurate performance of the proposed control structure, a SPS consisting of two VSCs is considered. A step PPL is carried out at t=60ms. The control system should be able to support the load in order of milliseconds. To preserve the properties of both $A - CC_{IT2}$ and $S - CC_{IT2}$, the $SI - IT2 - FPI$ controller with $M - CC_{IT2}$ has been adopted (by setting $\alpha = 0.5$) in this work. The coefficients embedded in the secondary voltage and frequency controllers are adjusted and set as $k_p = 0.01$ and $k_i = 1000$ and also the input $SF(k_e)$ and output $SF(k_u)$ are set to 1. It is worth to note that the conventional multi-loop control structures compensate for voltage and frequency deviations in order of multiple seconds [15]. However, based on the IEEE 1574 standard, allowable frequency deviations are 1% for under frequency and 0.8% for over frequency in the SPS and the allowable restoration time is 160 ms. The experimental setup is demonstrated in Fig. 5, where two Semikron 18 kW-VSCs are connected to the load trough the Schaffner LC filters.

The main achievement of the proposed control strategy is demonstrated in Fig. 6, where fast and accurate power sharing is carried on. By applying a PPL at t=60 ms, the controller shares active power between two VSCs very fast (Fig. 6). It worth to note that the

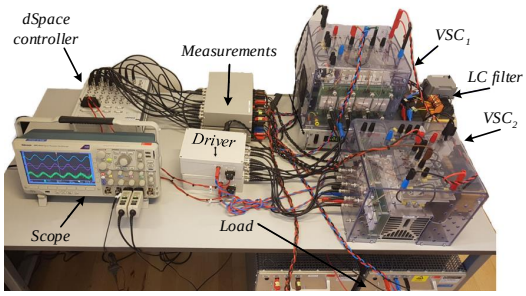

Fig. 5. Experimental setup.

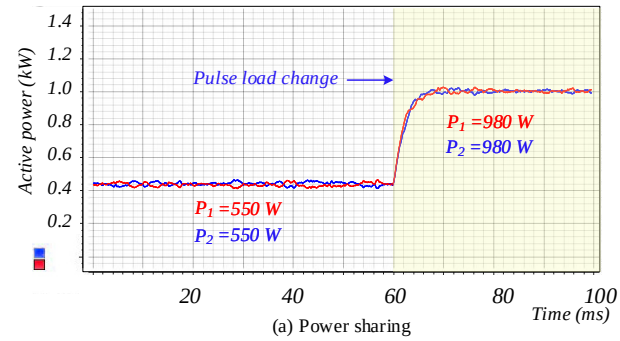

(a) Power sharing

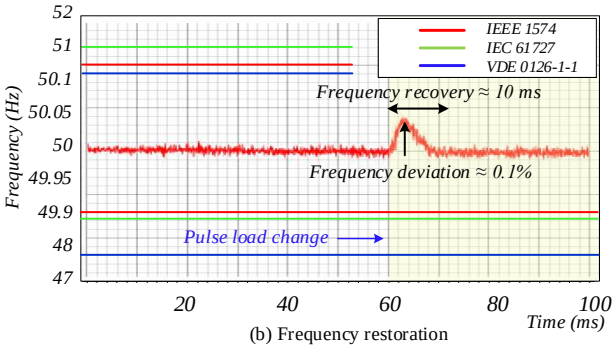

(b) Frequency restoration

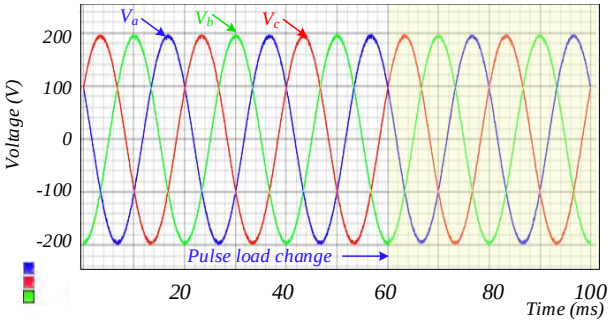

(c) Load voltage performance

Fig. 6. Validation of the proposed approach during a pulse load changes. (a) Transient power sharing accuracy between two VSCs. (b) SPS Frequency restoration and marginal standards. (c) Voltage amplitude of the VSCs at the load bus.

conventional linear control structures cannot share power accurately during the transient time, and accurate power sharing mostly carried on during several seconds [15].

Fig. 6 (b) shows the fast frequency regulation with the PPL at t=60 ms. Compared to the conventional control strategy presented in the literature (see Fig. 10 in [15]), the proposed control strategy compensates for frequency deviations order of magnitude faster than the state of the arts. Fig. 6 (c) shows the phase voltages of two VSCs at the load bus. As it can be seen, the voltages of VSCs

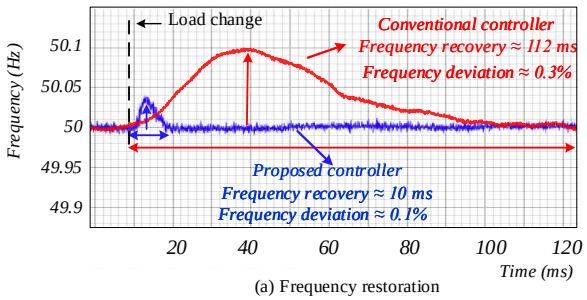

(a) Frequency restoration

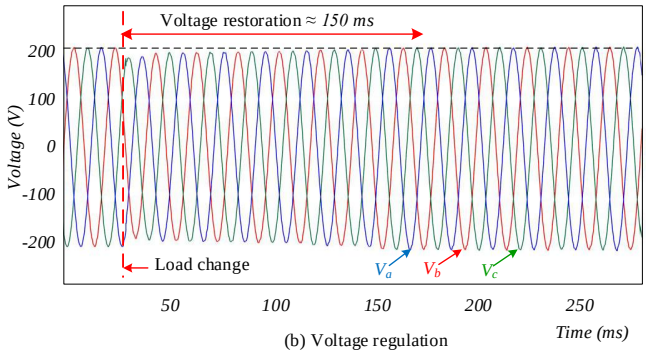

(b) Voltage regulation

Fig. 7. Performance of proposed control structure in comparison to the conventional cascaded linear control methods. (a) Frequency restoration (blue: proposed control approach, red: linear cascaded control); (b) Voltage regulation by employing linear control structure.

maintained stable during a load change. To validate the performance of the proposed control approach, a linear multi-loops control method, which is widely accepted in the literature and presented in [5], is implemented to serve as a benchmark. In this control structure, the inner current control loops tracks the command signal from the outer voltage control loop. These control loops are designed based on the serial tuning. Therefore, innermost current control loop the first to be tuned, and then outer voltage loop is designed with lower bandwidth to avoid undeniable interactions. Fig. 7 (a) shows the frequency restoration employing multi-loop control structure (red line) and proposed control structure (blue line). Obviously, the proposed controller compensates for frequency deviations far superior compared to the linear multi-loop control strategy. Fig. 7 (b) shows voltage regulation employing linear controllers. Compared to the proposed control structure (Fig. 6 (c)), dynamic performance of linear multi-loop controller is very slow.

VI. The Advantages of the Proposed Approach

The main goal of this study is to develop the control structure of the SPS with PPLs to compensate for the voltage and frequency deviations with much higher bandwidth. In the design of the control approach, considerations are made that have an essential role in the practical implementation.

1) The proposed control strategy is easy to implement with no difficulties with undesired control loops interactions.

2) In this control scheme, a single step prediction horizon is applied. Hence it has a light burden of computations. This feature is very crucial for online control cases and practical implementation.

3) The suggested control approach can be implemented in different SPS typologies with different loads, and grid configurations.

4) For the first time, a new SI-IT2-FPI algorithm has been introduced to compensate the voltage and frequency deviations at secondary control level.

VII. Conclusion

In this paper, a high bandwidth control structure for the SPS is proposed. Practically, the presented control strategy compensate for voltage and frequency deviations in order o magnitude faster than linear control structure shown in the literature. This approach is realized by replacing the FCS-MPC in the inner control loop to provide appropriate signaling for VSCs with higher bandwidth, then a SI-IT2-FPI algorithm is employed at the higher level to restore the SPS frequency and voltage with higher bandwidth. This modification significantly enhances the dynamic performance of the SPS. Experimental results verified the fast dynamic response of the proposed control structure with the PPL in an SPS with two VSCs.

References

[1] M.-H. Khooban, T. Dragicevic, F. Blaabjerg, and M. Delimar, "Shipboard microgrids: a novel approach to load frequency control," *IEEE Transactions on Sustainable Energy*, vol. 9, no. 2, pp. 843–852, 2018.

[2] R. Heydari, M. Alhasheem, T. Dragicevic, and F. Blaabjerg, "Model predictive control approach for distributed hierarchical control of vsc-based microgrids," in *EPE'18 ECCE Europe*. IEEE, 2018, pp. P–1.

[3] R. Heydari, T. Dragicevic, and F. Blaabjerg, "Coordinated operation of vscs controlled by mpc and cascaded linear controllers in power electronic based ac microgrid," in *19th Workshop on Control and Modeling for Power Electronics*. IEEE, 2018, pp. 1–4.

[4] F. Blaabjerg, R. Teodorescu, M. Liserre, and A. V. Timbus, "Overview of control and grid synchronization for distributed power generation systems," *IEEE Trans. on Ind. Electron.*, vol. 53, no. 5, pp. 1398–1409, Oct 2006.

[5] F. De Bosio, L. A. de Souza Ribeiro, F. D. Freijedo, M. Pastorelli, and J. M. Guerrero, "Effect of state feedback coupling and system delays on the transient performance of stand-alone vsi with lc output filter," *IEEE Trans. Ind. Electron*, vol. 63, no. 8, pp. 4909–4918, 2016.

[6] J. Rodriguez, J. Pontt, C. A. Silva, P. Correa, P. Lezana, P. Cortes, and U. Ammann, "Predictive Current Control of a Voltage Source Inverter," *IEEE Trans. on Ind. Electron.*, vol. 54, no. 1, pp. 495–503, Feb 2007.

[7] T. Dragičević, "Model predictive control of power converters for robust and fast operation of ac microgrids," *IEEE Transactions on Power Electronics*, vol. 33, no. 7, pp. 6304–6317, 2018.

[8] P. Acuna, L. Moran, M. Rivera, J. Dixon, and J. Rodriguez, "Improved active power filter performance for renewable power generation systems," *IEEE Trans. on Power Electron.*, vol. 29, no. 2, pp. 687–694, Feb 2014.

[9] T. Dragičević, R. Heydari, and F. Blaabjerg, "Super-high bandwidth secondary control of ac microgrids," in *Proc. IEEE APEC*, 2018, pp. 3036–3042.

[10] R. Heydari, A. Amiri, T. Dragicevic, P. Popovski, and F. Blaabjerg, "High bandwidth distributed secondary control with communication compensation in vsc-based microgrid," in *EPE'18 ECCE Europe*. IEEE, 2018, pp. P–1.

[11] R. Majumder, "Feasibility and challenges in microgrids for marine vessels," Ph.D. dissertation, Chalmers University of Technology, 2016.

[12] R. E. Hebner, F. M. Uriarte, A. Kwasinski, A. L. Gattozzi, H. B. Estes, A. Anwar, P. Cairoli, R. A. Dougal, F. Xianyong, C. Hung-Ming *et al.*, "Technical cross-fertilization between terrestrial microgrids and ship power systems," *Journal of Modern Power Systems and Clean Energy*, vol. 4, no. 2, pp. 161–179, 2016.

[13] T. Kumbasar, "Robust stability analysis and systematic design of single-input interval type-2 fuzzy logic controllers," *IEEE Transactions on Fuzzy Systems*, vol. 24, no. 3, pp. 675–694, 2016.

[14] A. Sarabakha, C. Fu, E. Kayacan, and T. Kumbasar, "Type-2 fuzzy logic controllers made even simpler: From design to deployment for uavs," *IEEE Transactions on Industrial Electronics*, vol. 65, no. 6, pp. 5069–5077, 2018.

[15] Q. Shafiee, C. Stefanovic, T. Dragicevic, P. Popovski, J. C. Vasquez, and J. M. Guerrero, "Robust networked control scheme for distributed secondary control of islanded microgrids," *IEEE Trans. Ind. Electron*, vol. 61, no. 10, pp. 5363–5374, 2014.